

# Impaired $\text{Cl}^-$ Extrusion in Layer V Pyramidal Neurons of Chronically Injured Epileptogenic Neocortex

Xiaoming Jin, John R. Huguenard, and David A. Prince

Department of Neurology and Neurological Sciences, Stanford University School of Medicine, Stanford, California

Submitted 16 July 2004; accepted in final form 23 November 2004

**Jin, Xiaoming, John R. Huguenard, and David A. Prince.** Impaired  $\text{Cl}^-$  extrusion in layer V pyramidal neurons of chronically injured epileptogenic neocortex. *J Neurophysiol* 93: 2117–2126, 2005; doi: 10.1152/jn.00728.2004. In the mature brain, the  $\text{K}^+/\text{Cl}^-$  cotransporter KCC2 is important in maintaining low  $[\text{Cl}^-]_i$ , resulting in hyperpolarizing GABA responses. Decreases in KCC2 after neuronal injuries result in increases in  $[\text{Cl}^-]_i$  and enhanced neuronal excitability due to depolarizing GABA responses. We used the gramicidin perforated-patch technique to measure  $E_{\text{Cl}}$  ( $\sim E_{\text{GABA}}$ ) in layer V pyramidal neurons in slices of partially isolated sensorimotor cortex of adult rats to explore the potential functional consequence of KCC2 downregulation in chronically injured cortex.  $E_{\text{GABA}}$  was measured by recording currents evoked with brief GABA puffs at various membrane potentials. There was no significant difference in  $E_{\text{Cl}}$  between neurons in control and undercut animals ( $-71.2 \pm 2.6$  and  $-71.8 \pm 2.8$  mV, respectively). However, when loaded with  $\text{Cl}^-$  by applying muscimol puffs at 0.2 Hz for 60 s, neurons in the undercut cortex had a significantly shorter time constant for the positive shift in  $E_{\text{Cl}}$  during the  $\text{Cl}^-$  loading phase ( $4.3 \pm 0.5$  s for control and  $2.2 \pm 0.4$  s for undercut,  $P < 0.01$ ). The positive shift in  $E_{\text{Cl}}$  3 s after the beginning of  $\text{Cl}^-$  loading was also significantly larger in the undercut group than in the control, indicating that neurons in undercut cortex were less effective in maintaining low  $[\text{Cl}^-]_i$  during repetitive activation of GABA<sub>A</sub> receptors. Application of furosemide eliminated the difference between the control and undercut groups for both of these measures of  $[\text{Cl}^-]_i$  regulation. The results suggest an impairment in  $\text{Cl}^-$  extrusion resulting from decreased KCC2 expression that may reduce the strength of GABAergic inhibition and contribute to epileptogenesis.

## INTRODUCTION

Increases in chloride conductance are a major factor underlying the effect of  $\gamma$ -aminobutyric acid (GABA) at GABA<sub>A</sub> receptors (Bormann et al. 1987). Whether activation of these receptors leads to hyperpolarization or depolarization depends principally on the relationship between the equilibrium potential for  $\text{Cl}^-$  ( $E_{\text{Cl}}$ ) and the resting membrane potential ( $V_m$ ). In the immature brain, where  $[\text{Cl}^-]_i$  is high and  $E_{\text{Cl}}$  is positive to  $V_m$ , activation of GABA<sub>A</sub> receptors causes  $\text{Cl}^-$  efflux and depolarizing inward current (Ben Ari et al. 1994; Cherubini et al. 1990; Kakazu et al. 1999; Luhmann and Prince 1991), whereas in the mature brain, low  $[\text{Cl}^-]_i$  and an  $E_{\text{Cl}}$  negative to  $V_m$  results in  $\text{Cl}^-$  influx and hyperpolarizing inhibitory postsynaptic potentials (IPSPs) during GABA<sub>A</sub> receptor activation (Andersen et al. 1980; Benardo 1994; Connors et al. 1988). This developmental shift indicates that  $[\text{Cl}^-]_i$  is not passively distributed across membranes, rather it is regulated

by the cation-chloride cotransporters and the  $\text{Cl}^-/\text{HCO}_3^-$  exchangers (Payne et al. 2003). The switch from depolarizing to hyperpolarizing GABA responses results from a decrease of  $[\text{Cl}^-]_i$  attributable to an increase in the  $\text{Cl}^-$  extruding  $\text{K}^+/\text{Cl}^-$  cotransporter, KCC2 (Kakazu et al. 1999; Mikawa et al. 2002; Plotkin et al. 1997; Rivera et al. 1999) and a decrease in the  $\text{Cl}^-$  accumulating  $\text{K}^+/\text{Na}^+/\text{Cl}^-$  cotransporter, NKCC1 (Clayton et al. 1998; Marty et al. 2002; Yamada et al. 2004).

In pathophysiological conditions such as neuronal injuries, the effect of GABA<sub>A</sub> receptor activation can change from hyperpolarization to depolarization due to a decrease in KCC2 and consequent increases in  $[\text{Cl}^-]_i$  (Coull et al. 2003; Malek et al. 2003; Nabekura et al. 2002; Toyoda et al. 2003). After trauma, activation of GABA<sub>A</sub> receptors causes depolarization and an increase in intracellular  $\text{Ca}^{2+}$  in different CNS regions (Nabekura et al. 2002; Toyoda et al. 2003; van den Pol et al. 1996). In brain slice preparations, tetanic stimulation switches the response to GABA from inhibition to one of excitation as a result of an increase in  $[\text{K}^+]_o$ , which probably disturbs  $\text{Cl}^-$  extrusion (DeFazio et al. 2000; McCarran and Alger 1985; Taira et al. 1997). Kindling-induced or spontaneous seizures can also lead to reductions in expression of KCC2 (Rivera et al. 2002) and increases in NKCC1 (Okabe et al. 2002).

Normal brain function depends on a delicate balance between excitatory and inhibitory synaptic activity. Results from a variety of experiments indicate that reductions in cortical inhibitory electrogenesis can induce epileptiform activity (Prince 1999). Reductions in inhibition, such as might result from decreases in numbers of GABAergic neurons (Buckmaster and Jongen-Relo 1999; Dinocourt et al. 2003; Magloczky et al. 2000), loss of inhibitory synapses (Bloom and Iversen 1971; Ribak et al. 1982), and alterations in GABA<sub>A</sub> receptors (Bianchi et al. 2002; Rice et al. 1996; Wallace et al. 2001), can lead to hyperexcitability in neuronal networks and may be one underlying mechanism in epileptogenesis (Bernard et al. 2000; Prince 1999; Sloviter 1987). Small reductions in the strength of cortical GABAergic inhibition have been reported in chronic models of epilepsy (Li and Prince 2002; Roper et al. 1997), and pharmacologically induced disinhibition can result in epileptiform discharges in acute experiments (Chagnac-Amitai and Connors 1989; Schwartzkroin and Prince 1978).

Potential contributions of disordered  $\text{Cl}^-$  transport to the epileptogenesis occurring after neocortical trauma have not been well explored. Epileptogenesis is known to occur in vivo in partially isolated islands of neocortex of cats (Echlin and Battista 1963), monkey (Sharpless and Halpern 1962) and

Address for reprint requests and other correspondence: D. A. Prince, Neurology and Neurological Sciences, Stanford University School of Medicine, Room M016, Stanford, CA 94305-5122 (E-mail: daprince@stanford.edu).

The costs of publication of this article were defrayed in part by the payment of page charges. The article must therefore be hereby marked "advertisement" in accordance with 18 U.S.C. Section 1734 solely to indicate this fact.

perhaps human (Scoville 1960) 2–3 wk after injury. We have adapted this model to guinea pig and rat and shown that both spontaneous and evoked interictal epileptiform activity and rare ictal episodes can occur in neocortical slices cut through the partially isolated cortical island and maintained *in vitro* (Hoffman et al. 1994; Prince and Tseng 1993; Salin et al. 1995). Preliminary results obtained with immunocytochemical and *in situ* hybridization techniques have shown that KCC2 protein and mRNA are downregulated in layer V pyramidal neurons of rat partially isolated “undercut” neocortex beginning ~2 wk after injury (Prince et al. 2000; I. Parada and D. A. Prince, unpublished data). The effects of reductions in KCC2 on  $[Cl^-]_i$ , resting  $E_{Cl}$ , and the capacity of these neurons to recover from increases in  $[Cl^-]_i$  that result from intense activation of GABA<sub>A</sub> receptors, have not been examined in this model of posttraumatic epileptogenesis. To explore these potential physiological consequences of reduced KCC2 expression, we applied the perforated-patch technique to pyramidal cells in layer V of control and chronically injured, partially isolated neocortex. We expected that the decreased expression of KCC2 after injury would result in a positive shift in  $E_{Cl}$  and/or slower  $Cl^-$  clearance, which could contribute to the increased excitability and epileptogenesis.

## METHODS

### *Surgical procedures*

All experiments were carried out according to protocols approved by the Stanford Institutional Animal Care and Use Committee. Forty-four Sprague-Dawley rats aged P36–46 (P0 = date of birth) were used for *in vitro* recordings. Partially isolated islands of sensory-motor cortex (“undercuts”) were produced in 26 anesthetized rats at P21, using previously described techniques (Hoffman et al. 1994; Li and Prince 2002). Rats were deeply anesthetized with ketamine (80 mg/kg ip) and xylazine (Rompun, 8 mg/kg ip) and mounted in a stereotaxic frame; the scalp was incised and retracted, and a portion of frontoparietal cortex of the left hemisphere was exposed by removing a ~3 × 5 mm bone window centered on the coronal suture, leaving the dura intact. A partial isolation of an island of sensory-motor cortex (Zilles 1985) was made as previously described (Hoffman et al. 1994). A 30-gauge needle, bent at approximately a right angle 2.5–3 mm from the tip, was inserted tangentially through the dura, just beneath the pial vessels, parasagittally ~1–2 mm from the interhemispheric sulcus, and lowered to a depth of 2 mm. The needle then was rotated 120–135° to produce a contiguous white matter lesion, elevated to a position just beneath the pia, making a second transcortical cut, and removed. An additional transcortical lesion was placed ~2 mm lateral and parallel to the parasagittal cut in a similar manner. The skull opening was then covered with sterile plastic wrap (Saran Wrap), and the skin sutured. Rats were allowed to recover for ≥2 wk, a latency at which most *in vitro* slices containing a portion of the injured area generated evoked epileptiform activity in previous experiments (Graber and Prince 1999; Hoffman et al. 1994).

### *Slice preparation and recording*

Animals were anesthetized with pentobarbital (55 mg/kg ip) and decapitated; the brain was rapidly removed and placed in cold (4°C) oxygenated slicing solution containing (in mM) 230 sucrose, 2.5 KCl, 1.25 NaH<sub>2</sub>PO<sub>4</sub>, 10 MgSO<sub>4</sub>·7H<sub>2</sub>O, 10 glucose, 0.5 CaCl<sub>2</sub>·2H<sub>2</sub>O, and 26 NaHCO<sub>3</sub>. Coronal slices (250 μm) were cut with a vibratome (Lancer Series 1000) through the lesioned cortex and from the same region in control animals, and maintained using standard techniques (Li and Prince 2002). After ~1 h incubation at 36°C in standard

artificial cerebrospinal fluid (ACSF), slices were held at room temperature. The ACSF contained (in mM) 126 NaCl, 2.5 KCl, 1.25 NaH<sub>2</sub>PO<sub>4</sub>, 2 CaCl<sub>2</sub>, 2 MgSO<sub>4</sub>·7H<sub>2</sub>O, 26 NaHCO<sub>3</sub>, and 10 glucose; pH 7.4 when saturated with 95% O<sub>2</sub>-5% CO<sub>2</sub>. Bicarbonate is known to make a small contribution to the GABA equilibrium potential (Bormann et al. 1987) that might be eliminated through the use of bicarbonate-free ACSF. We assumed that the presence of bicarbonate in our experiments would affect  $E_{Cl}$  similarly in control and undercut neurons recorded under identical conditions, and therefore standard ACSF was used as in the preceding text, to record  $E_{GABA}$  under physiological conditions. We also corrected the contribution of bicarbonate current in our calculations using Goldman-Hodgkin-Katz equation (GHK equation).

Patch electrodes were pulled from borosilicate glass tubing (1.5 mm OD), and those used for gramicidin perforated patch recordings had an impedance of 2–3 MΩ when filled with intracellular solution containing (in mM) 130 KCl, 5 EGTA, 0.5 CaCl<sub>2</sub>·2H<sub>2</sub>O, 2 MgCl<sub>2</sub>·6H<sub>2</sub>O, and 10 HEPES, pH 7.3 adjusted with 1 M KOH. Gramicidin at a final concentration of 25–50 μg/ml was added to the pipette solution before each experiment and the mixture sonicated for ≥30 s. Pipettes for whole cell recording had an impedance of 2.5–4 MΩ when filled with intracellular solution containing (in mM) 95 K-gluconate, 40 KCl, 5 EGTA, 0.2 CaCl<sub>2</sub>·2H<sub>2</sub>O, and 10 HEPES, pH 7.3 adjusted with 1 M KOH. The osmolarity of the pipette solutions was adjusted to 275–285 mosM. Liquid junction potentials were determined using the junction potential calculator in Clampex 9.0 software and corrected during data analysis. Single slices were transferred to a recording chamber where they were minimally submerged and maintained at 32 ± 1°C. Patch-clamp recordings were made from visually identified layer V pyramidal cells in undercut cortex or the same region in control slices, using infrared video microscopy and a ×63 water-immersion lens with differential interference contrast optics (Zeiss Axioskop) and an Axopatch 200A amplifier (Axon Instruments). Access resistance was measured in voltage-clamp mode from responses to 5 mV depolarizing voltage pulses. Perforated patch recordings with access resistance of <80 MΩ and without significant (>25%) changes during the recording were used for data analysis. The responses were low-pass filtered at 2 kHz and recorded on hard disk for later analysis.

### *Drug application*

Drugs were delivered using a local perfusion system composed of eight fine tubes ending in a common outlet tube, positioned ~250 μm from the recorded neuron (Kumar et al. 2002; Sun et al. 2001). CGP35348 0.5 mM, TTX 1 μM, muscimol 100 μM, GABA 100 μM, furosemide 0.5 mM, bumetanide 10 μM were mixed in ACSF and locally perfused. All drugs were obtained from Sigma.

To activate GABA<sub>A</sub> receptors, brief pressure pulses (“puffs”; 12–15 ms, 200–275 kPa) of GABA (100 μM) or muscimol (100 μM) were applied to the soma of the recorded neuron through a patch pipette located ~50–80 μm away in layer V. Pipettes for pressure applications were fabricated as described in the preceding text for patch pipettes, and had an impedance of 5–7 MΩ when filled with ACSF containing GABA or muscimol. The distance between the “puffer” pipette and soma was routinely adjusted to evoke minimally detectable current responses. Pressure pulses were applied using a solenoid-controlled pressure valve. The settings were kept constant during recording.

### *Data analysis*

Data were analyzed using Clampfit 9.0 (Axon Instruments, Union City, CA) and Origin (Microcal Software, Northampton, MA) software. Perforated-patch access resistance was determined by analyzing the transient responses to 5 mV voltage-clamp steps (Marty and Neher 1985). The amplitude of the voltage step divided by the resultant instantaneous current yielded an estimate of access resistance. “In-

stantaneous" current was measured as the extrapolated zero time current obtained after fitting two exponential functions to the decay of the capacitive current transients. All membrane potentials were subsequently corrected for the voltage drop across the access resistance. In experiments involving GABA puffs, equilibrium potentials were determined by measuring the voltage at the intersection of the holding and total current  $I$ - $V$  curves. When voltage ramps were used, chloride reversal potentials were determined by measuring the voltage at the intersection of the control and muscimol-induced current curves.

Once a stable perforated patch was established, passive membrane properties were determined from voltage responses to small 100 pA current steps (Rall 1977). The membrane time constant ( $\tau_m$ ) was estimated from the slowest component of multiexponential fits to the voltage responses from the onset to the steady state. The electrotonic length ( $L$ ) and dendritic dominance ( $\rho$ ) were further calculated based on result of multiexponential fits.

To quantify  $\text{Cl}^-$  load, we integrated the total  $\text{Cl}^-$  loading current, both during the holding period at  $-50$  mV and during the voltage ramp, by subtracting net inward  $\text{Cl}^-$  current from outward  $\text{Cl}^-$  current (Fig. 2B3). The contribution of  $\text{HCO}_3^-$  current was estimated by applying the GHK equation, using a  $\text{Cl}^-$ : $\text{HCO}_3^-$  permeability ratio of 0.8:0.2 (Kaila et al. 1993; Staley et al. 1995) and assuming that  $[\text{Cl}^-]_i$  and  $\text{Cl}^-$  cotransporter activity did not change significantly during each ramp. The total  $\text{Cl}^-$  load over the 60 s period (total charge) was used to estimate the number of ions transferred

$$[\text{Cl}^-]_{\text{influx}} = Q_{\text{total}}/F$$

Where  $F$  is Faraday's constant, and  $Q_{\text{total}}$  is the total  $\text{Cl}^-$  load over the 60 s period.

The shifts in  $[\text{Cl}^-]_i$  in the first three ramps were individually calculated from the modified GHK equation, using the change in  $E_{\text{GABA}}$  during each ramp period. Neuronal volume was then estimated from the number of ions (moles) admitted versus the change in  $[\text{Cl}^-]_i$  during each of the three ramp periods and averaged (Staley and Proctor 1999)

$$\text{Cell volume} = \Delta[\text{Cl}^-]_{\text{influx}}/\Delta[\text{Cl}^-]_i$$

Where  $\Delta[\text{Cl}^-]_{\text{influx}}$  is moles of  $\text{Cl}^-$  loaded during a single ramp, and  $\Delta[\text{Cl}^-]_i$  is the change in intracellular  $\text{Cl}^-$  concentration during that ramp period.

Unless otherwise indicated, statistical analyses were performed using Student's  $t$ -test with a level of significance of  $P < 0.05$ . Data are presented as means  $\pm$  SE.

## RESULTS

All recordings were obtained from layer V within the partially isolated cortex and from homologous areas of control cortex from age-matched untreated animals. Transcortical cuts were easily seen in slices under a low power objective. Undercutting lesions were present in white matter closely adjacent to layer VI and a small area of cavitation was often associated with the undercut. Layer V pyramidal neurons were visually identified based on their location, large pyramidal-shaped somata and a single emerging apical dendrite extending toward the pial surface. Data from neurons with a resting membrane potential more negative than  $-50$  mV were accepted for analysis. Most neurons had a regular spiking firing pattern in response to depolarizing current pulses (83.4%); the remainder were burst firing pyramidal neurons (Connors et al. 1982; Tseng and Prince 1996). Data from these two groups of cells were not significantly different and therefore were combined for analysis. Because the  $\text{GABA}_A$  equilibrium potential ( $E_{\text{GABA}}$ ) is predominately determined by  $E_{\text{Cl}}$ , we refer to  $E_{\text{GABA}}$  as  $E_{\text{Cl}}$  throughout.

### Resting $E_{\text{Cl}}$ in layer V pyramidal neurons of undercut epileptogenic cortex

Acceptable perforated patch-clamp recordings were obtained from 13 neurons in 12 slices of undercut cortex from seven rats and 8 cells in 8 slices of control cortex from four rats. CGP 35348 (0.5 mM) and TTX (1  $\mu\text{M}$ ) were locally perfused to block  $\text{GABA}_B$  receptor activation and action potential firing respectively. GABA (100  $\mu\text{M}$ ) was pressure-applied close to the soma of the voltage-clamped cells. An example of a perforated patch-clamp experiment is shown in Fig. 1A. The agonist-induced current was measured at different command potentials between  $-90$  and  $-20$  mV. After correction for access resistance, current-voltage ( $I$ - $V$ ) relationships before and during the GABA response revealed the GABA reversal potential ( $E_{\text{GABA}}$ , Fig. 1B,  $\leftarrow$ ). The mean  $E_{\text{GABA}}$  was  $-71.2 \pm 2.6$  mV ( $n = 8$ ) in the control group and  $-71.8 \pm 2.8$  mV ( $n = 13$ ) in the undercut group (Fig. 1C). These  $E_{\text{GABA}}$  levels were hyperpolarizing relative to the average membrane potential of  $-58.8 \pm 2.4$  and  $-63.7 \pm 2.3$  mV for the control and undercut groups, respectively. The calculated mean intracellular chloride concentrations in control and undercut neurons under these conditions were  $5.4 \pm 1.0$  and  $5.6 \pm 1.2$  mM, respectively, using the modified GHK equation with  $[\text{HCO}_3^-]_o = 26$  mM,  $[\text{HCO}_3^-]_i = 16$  mM (Dallwig et al. 1999) and  $P_{\text{HCO}_3^-}/P_{\text{Cl}^-} = 0.25$  (Kaila et al. 1993; Staley et al. 1995). There were no statistical differences between the control and undercut groups in either  $E_{\text{GABA}}$  or calculated  $[\text{Cl}^-]_i$  (Fig. 1C).

### Changes in $E_{\text{Cl}}$ during $\text{Cl}^-$ loading in neurons of undercut cortex

The lack of a significant difference in  $E_{\text{GABA}}$  ( $E_{\text{Cl}}$ ) between the undercut and control group was surprising because previous experiments have shown decreased KCC2 immunoreactivity in neurons of layer V of undercut cortex (Prince et al. 2000; D. A. Prince, unpublished data) and decreased KCC2 expression resulting in a positive shift in  $E_{\text{Cl}}$  and depolarizing  $\text{GABA}_A$  responses has been reported after axotomy, other neuronal injuries, and seizures (Malek et al. 2003; Nabekura et al. 2002; Woo et al. 2002). It is possible that sufficient KCC2 activity is present in neurons of the undercut cortex to maintain a normal low  $[\text{Cl}^-]_i$  under resting conditions but not during periods of  $\text{Cl}^-$  loading resulting from GABA release during intense interneuronal discharge as might occur during epileptiform activity (e.g., Fig. 11 in McCormick et al. 1985). To further explore this issue, we held  $V_m$  of neurons at  $-50$  mV and induced  $\text{Cl}^-$  loading by applying 100  $\mu\text{M}$  muscimol puffs to the somata of layer V pyramidal neurons at 0.2 Hz for 60 s to mimic the effect of intense  $\text{GABA}_A$  receptor activation (Thompson and Gahwiler 1989). Voltage ramps from  $-100$  to  $-40$  mV were applied at 1 Hz to monitor the changes in membrane conductance over time during the loading and recovery phase (Fig. 2A).  $E_{\text{Cl}}$  was determined from voltage at the intersection of the control and muscimol current traces after correction for access resistance (Fig. 2B). In each cell, the time constant of changes in  $E_{\text{Cl}}$  during the loading phase and the recovery phase was obtained by fitting values for  $E_{\text{Cl}}$  from voltage ramp responses with a single-exponential function (Fig. 2C). Acceptable perforated patch-clamp recordings were obtained from 12 neurons in 10 slices of undercut cortex from seven rats and 8 cells in 6 slices of control cortex from five rats.

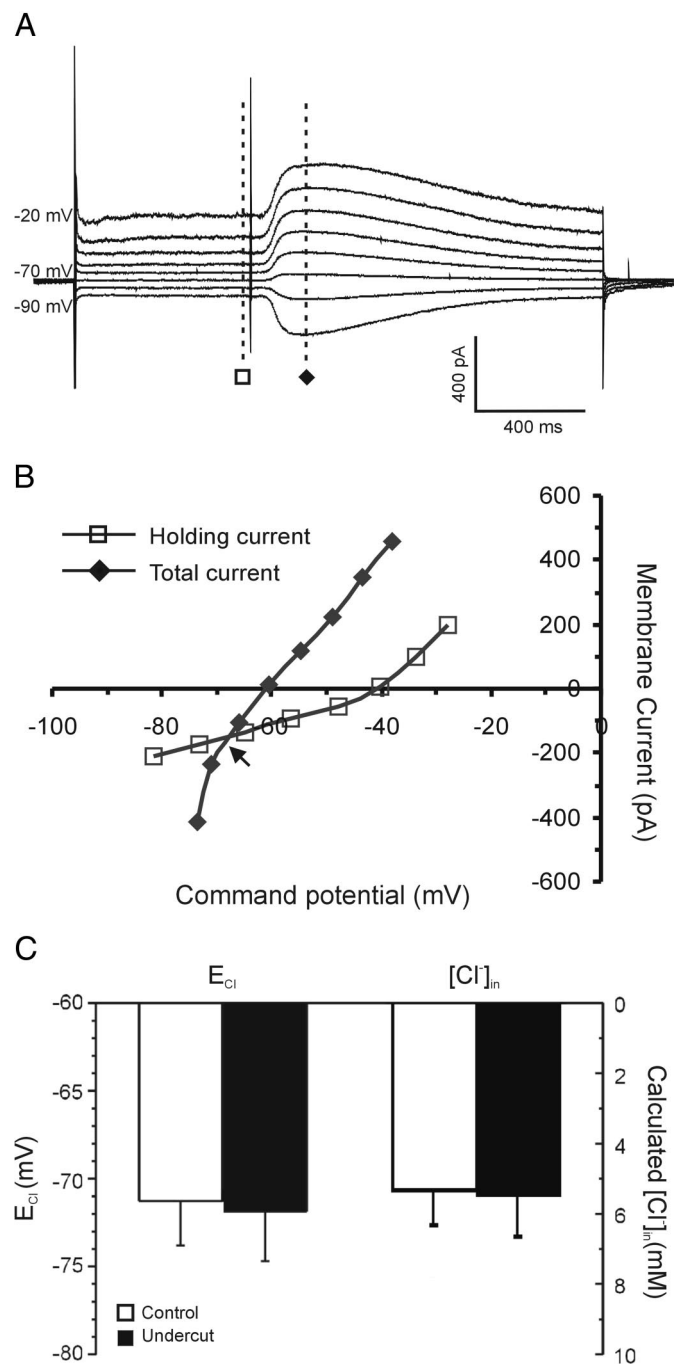


**FIG. 1.** Measurement of  $E_{Cl}$  using perforated patch-clamp recordings. **A:** gramicidin perforated patch-clamp recording of membrane currents evoked by brief (12 ~ 15 ms) focal GABA puffs (100  $\mu$ M) at different command potentials (-90 to -20 mV) in a layer V pyramidal neuron. TTX (1  $\mu$ M) and CGP35348 (0.5 mM) were continuously applied by local perfusion. Holding current ( $\square$ ) and peak current ( $\blacksquare$ ) were measured at times indicated by vertical dashed line. **B:**  $I$ - $V$  relationship of holding current and total current during GABA application in the same neuron. Arrow, GABA current reversal potential that is assumed to be  $\sim E_{Cl}$  (-68.6 mV in this neuron). **C:** resting  $E_{Cl}$  was unaltered in layer V pyramidal neurons of undercut epileptogenic cortex. Graphs show average  $E_{Cl}$  (left) and calculated  $[Cl^-]_{in}$  (right) in control and undercut groups.  $E_{Cl}$  was  $-71.2 \pm 2.6$  mV in control ( $\square$ ,  $n = 8$ ) and  $-71.8 \pm 2.8$  mV in undercut group ( $\blacksquare$ ,  $n = 13$ );  $[Cl^-]_{in}$ , calculated from the modified GHK equation, was  $5.4 \pm 1.0$  mM in control and  $5.6 \pm 1.2$  mM in undercut group. Differences between the 2 groups were not significant.

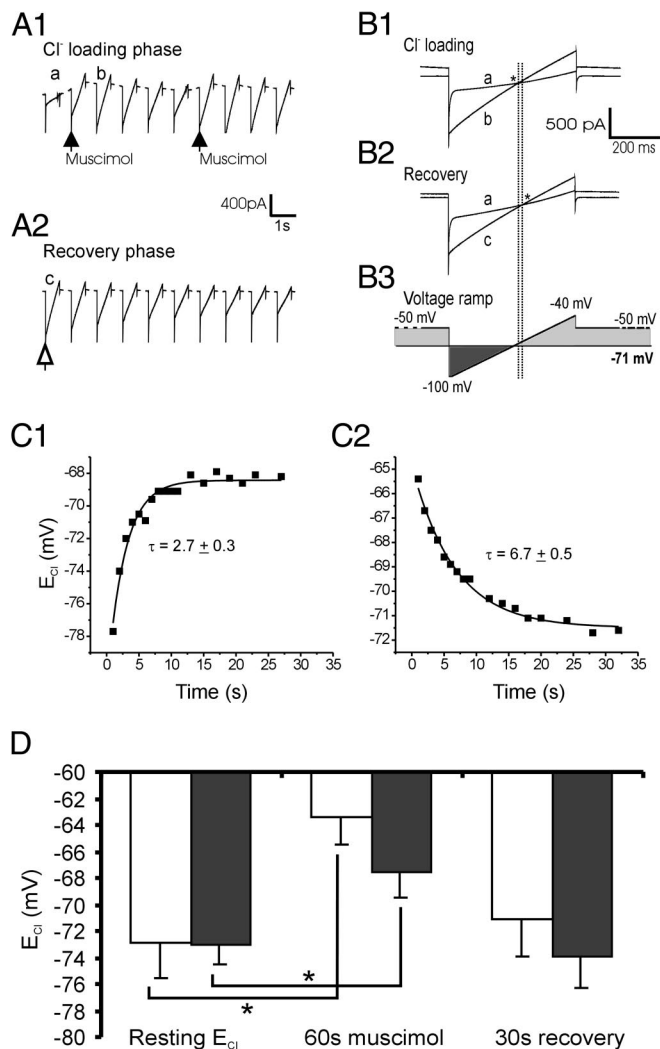


**FIG. 2.** Measurement of time constants for altered  $E_{Cl}$  during  $Cl^-$  loading and recovery. **A:** layer V pyramidal neuron voltage-clamped at -50 mV during application of 12 ~ 15 ms, 100  $\mu$ M muscimol pressure pulses (0.2 Hz) for 60 s to load  $Cl^-$ . Deflections show membrane current responses to voltage ramps as shown in **B**, delivered at 1 Hz. **A1:**  $Cl^-$  loading phase. Black arrows mark times of 1st and 2nd muscimol applications. **A2:** recovery phase, beginning immediately after last muscimol puff. Open arrowhead marks beginning of recovery phase. **B:**  $E_{Cl}$  was measured from intersection of currents evoked by voltage ramps. **B1:** superimposed responses obtained at points a and b of  $Cl^-$  loading phase in **A1**, before and immediately after 1st muscimol puff. **B2:** responses to same voltage ramp during recovery phase after last muscimol puff (response c in **A2**) and the control trace (response a in **A1**) were superimposed. Voltages at intersections of the control and muscimol response traces (asterisks) indicate the reversal potential at the beginning of  $Cl^-$  loading (**B1**) and the beginning of recovery phase (**B2**). **B3:** voltage ramp protocol used in **A** and **B** included 250 ms at -50 mV before and after a ramp ranging from -100 to -40 mV over 500 ms. The horizontal line drawn at -71 mV indicates  $E_{GABA}$ . The time spent at membrane voltages positive to  $E_{GABA}$  (light gray) was much greater than the time spent at more negative potentials (dark gray), leading to net  $Cl^-$  loading during the protocol. Vertical lines in **B**, **1**-**3**, indicate GABA reversal potential. **C:** time constants for  $E_{Cl}$  changes during and after  $Cl^-$  loading.  $E_{Cl}$  from a layer V pyramidal neuron in undercut cortex plotted as a function of time from the beginning of muscimol puff 30 s (**C1**) and from the beginning of recovery period (**C2**). Plots fit with a single-exponential function (solid lines). Tau is  $2.7 \pm 0.3$  s for loading phase and  $6.7 \pm 0.5$  s for recovery phase. **D:** changes in  $E_{Cl}$  during  $Cl^-$  loading and recovery phases. There were no significant differences between the 2 groups in resting  $E_{Cl}$  (left),  $E_{Cl}$  after 60 s of  $Cl^-$  loading (middle), or 30 s into the recovery period (right). The difference in  $E_{Cl}$  between the resting state and after 60 s of  $Cl^-$  loading was significant for both control and undercut groups (\*:  $P < 0.05$ ).

In both control and undercut groups, there was a significant positive shift in  $E_{\text{Cl}}$  between the resting state and after  $\text{Cl}^-$  loading (Fig. 2D), indicating that the muscimol loading protocol was effective in increasing  $E_{\text{Cl}}$ . The mean total  $\text{Cl}^-$  loading in 60 s, calculated based on total net inward current after correction for bicarbonate current according to GHK equation, was  $0.35 \pm 0.09$  and  $0.41 \pm 0.09$  femtomole in the control and undercut group, respectively. From the change in  $[\text{Cl}^-]_i$  derived from the  $\text{Cl}^-$  load, the mean cell volumes estimated were  $3,200 \pm 600$  and  $2,400 \pm 300 \mu\text{m}^3$  in the control and undercut group, respectively. Neurons in the undercut cortex tended to be smaller than control, but there were no statistical differences between the two groups in either  $\text{Cl}^-$  loading or cell volume ( $P > 0.05$ ). There were also no significant differences between the two groups in average  $E_{\text{Cl}}$  at the beginning and the end of  $\text{Cl}^-$  loading, and after 30 s recovery ( $P > 0.05$ , Fig. 2D).  $E_{\text{Cl}}$  at the beginning of  $\text{Cl}^-$  loading (measured at the beginning of the 1st muscimol puff) was  $-72.8 \pm 2.7$  and  $-73.1 \pm 2.4$  mV for the control and undercut groups, respectively, values very close to those for resting  $E_{\text{Cl}}$  measured using GABA puffs, as shown in Fig. 1C. Additionally, there was no significant difference in tonic GABA<sub>A</sub> currents between the two groups as estimated from baseline shifts in holding current after application of 10  $\mu\text{M}$  bicuculline (data not shown).

In comparison to the control group, the undercut group had faster  $\text{Cl}^-$  loading (Fig. 3, A and B;  $\tau = 4.3 \pm 0.5$  s,  $n = 6$  for control and  $2.2 \pm 0.4$  s,  $n = 11$  for undercut,  $P < 0.01$ ), but there was no significant difference between the two groups during the recovery phase. Further analysis of  $E_{\text{Cl}}$  change revealed that the shift in  $E_{\text{Cl}}$  3 s after the beginning of  $\text{Cl}^-$  loading was significantly larger in the undercut group than in the control (Fig. 3C;  $2.3 \pm 0.5$  mV,  $n = 8$  in control group and  $4.0 \pm 0.5$  mV,  $n = 12$  in undercut group;  $P < 0.05$ ), indicating that layer V pyramidal neurons in undercut cortex were less effective in maintaining a stable low level of  $[\text{Cl}^-]_i$  during sustained activation of GABA<sub>A</sub> receptors.

To rule out the possibility that the difference in  $\text{Cl}^-$  loading was in some way due to a change in intrinsic neuronal properties, we compared properties of neurons in control and undercut groups (Table 1). No significant differences were present in resting membrane potential ( $V_m$ ), electrotonic length ( $L$ ), dendritic dominance ( $p$ ), and input resistance ( $R_{\text{input}}$ ), although  $R_{\text{input}}$  tended to be higher in the undercut group. The membrane time constant ( $\tau_m$ ) was significantly longer in neurons of the undercut ( $52.9 \pm 5.8$  ms) than in control cells ( $31.6 \pm 3.2$  ms;  $P < 0.01$ ), suggesting an increase in membrane specific resistivity or capacitance in the undercut neurons. The changes in  $R_{\text{input}}$  and  $\tau_m$  were similar to those reported in earlier experiments (Prince and Tseng 1993). There was also no significant difference in peak GABA<sub>A</sub> conductance ( $G_{\text{GABA}}$ ) between control and undercut groups, suggesting that the undercut lesion did not result in a significant net change in the effects of GABA<sub>A</sub> receptor activation.

One explanation for the shorter time constant and larger amplitude of the shift in  $E_{\text{Cl}}$  at 3 s during the  $\text{Cl}^-$  loading phase would be an impaired  $\text{Cl}^-$  extrusion mechanism. To test this possibility, we applied the nonspecific  $\text{Cl}^-$  cotransporter blocker, furosemide, which affects both NKCC1 and KCC2. Because the inward  $\text{Cl}^-$  cotransporter NKCC1 has a primarily dendritic localization in adult cortical neurons and is not significantly involved in somatic  $\text{Cl}^-$  regulation (Martina et al.

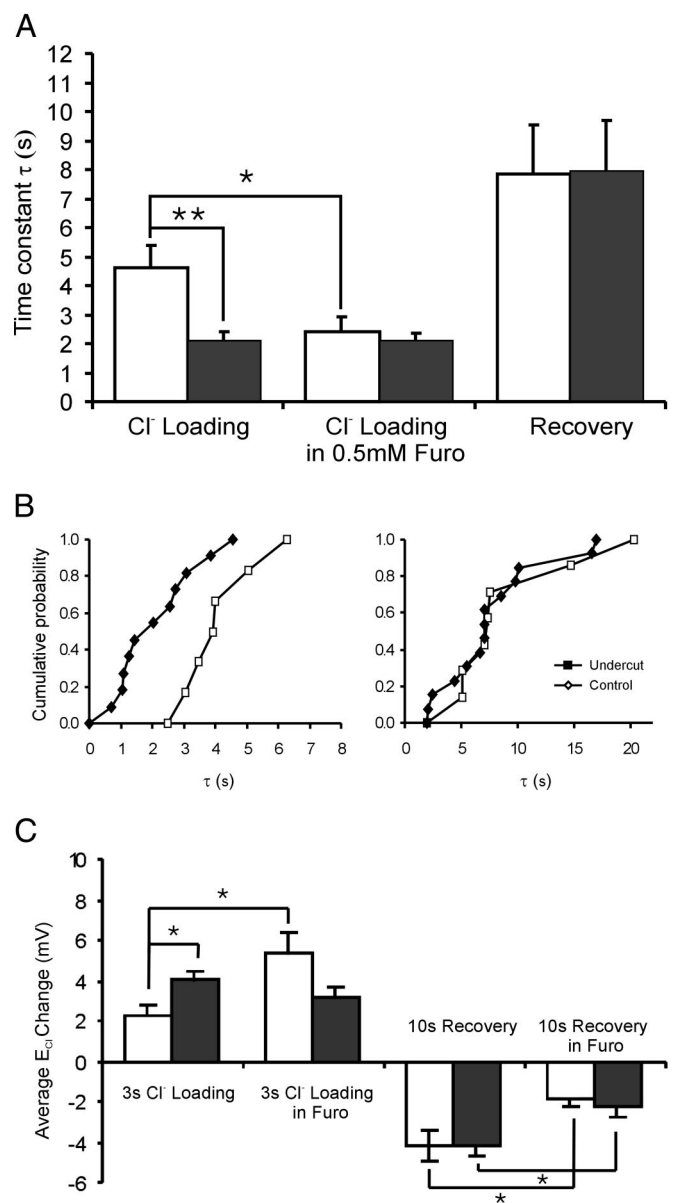


FIG. 3.  $E_{\text{Cl}}$  increases more rapidly in undercut cortical neurons than controls during  $\text{Cl}^-$  loading. A: graphs showing average time constants for  $\text{Cl}^-$  loading (left) and  $\text{Cl}^-$  loading in 0.5 mM furosemide (middle), and for  $\text{Cl}^-$  recovery (right). Average time constants for undercut and control groups during  $\text{Cl}^-$  loading phase were  $4.3 \pm 0.5$  s for control ( $n = 6$ ) and  $2.2 \pm 0.4$  s for undercut ( $n = 11$ , \*\*,  $P < 0.01$ ). There were no significant differences in time constants during  $\text{Cl}^-$  loading phase in 0.5 mM furosemide (middle) and during recovery phase between the control and undercut groups (right). In the control group, average time constant during  $\text{Cl}^-$  loading phase became faster (middle,  $\tau = 2.4 \pm 0.6$  s, \*,  $P < 0.05$ ) when 0.5 mM furosemide was present. B: cumulative probability plots for time constants of  $E_{\text{Cl}}$  change during  $\text{Cl}^-$  loading (left) and recovery phase (right) in both groups. Each data point represents the fraction of neurons in the group with tau that is equal to or less than the corresponding value shown on the x axis. The leftward shift of the curves during  $\text{Cl}^-$  loading phase in undercut group indicates significantly shorter time constants. C: average  $E_{\text{Cl}}$  change 3 s after the beginning of  $\text{Cl}^-$  loading phase and 10 s after the beginning of recovery phase during perfusion of normal artificial cerebrospinal fluid (ACSF) and ACSF containing 0.5 mM furosemide. There was a significant difference between control and undercut group during first 3 s of  $\text{Cl}^-$  loading phase (3 s  $\text{Cl}^-$  loading, \*,  $P < 0.05$ ), but not when 0.5 mM furosemide was added (3 s  $\text{Cl}^-$  loading in furo), or during the recovery phase. 0.5 mM furosemide resulted in a significant increase in  $E_{\text{Cl}}$  positive shift in control group during the loading phase ( $P < 0.05$ ) as well as in both groups during the 1st 10 s of the recovery phase.

TABLE 1. Membrane properties of control and undercut neurons

Group	$V_m$ , mV	$E_{GABA_A}$ , mV	$G_{GABA_A}$ , nS	$R_{input}$ , M $\Omega$	$L$	$\tau_m$ , ms	$\rho$
Control	$-63.1 \pm 2.7$ (16)	$-71.5 \pm 1.9$ (16)	$11.1 \pm 2.7$ (16)	$172.7 \pm 22.0$ (16)	$1.3 \pm 0.2$ (16)	$31.6 \pm 3.2$ (16)	$1.4 \pm 0.3$ (14)
Undercut	$-65.9 \pm 1.8$ (24)	$-72.4 \pm 1.6$ (24)	$12.9 \pm 1.6$ (24)	$185.5 \pm 18.9$ (22)	$1.5 \pm 0.2$ (18)	$52.9 \pm 5.8$ (18)**	$1.3 \pm 0.1$ (17)

Number of neurons is in parentheses. Values are presented as means  $\pm$  SE.  $V_m$ , membrane potential;  $E_{GABA_A}$ , GABA<sub>A</sub> equilibrium potential;  $G_{GABA_A}$ , GABA<sub>A</sub> conductance;  $R_{input}$ , input resistance;  $L$ , electrotonic length,  $\tau_m$ , membrane time constant;  $\rho$ , dendritic dominance; \*\*  $P < 0.01$ .

2001; and see following text), changes induced by furosemide would be due primarily to effects on KCC2 activity. Furosemide had no effect on the time constant for Cl<sup>-</sup> loading in undercut neurons (Fig. 3A). However, in the control group, addition of 0.5 mM furosemide resulted in a significant decrease in time constant (Fig. 3A, middle) and a significant increase in Cl<sup>-</sup> loading (Fig. 3C, 3 s Cl<sup>-</sup> loading in furo). Thus blockade of KCC2 with furosemide interfered with the normal extrusion of intracellular Cl<sup>-</sup> in control but had no effect in undercut cells. Furosemide also eliminated the difference between the undercut and control groups in Cl<sup>-</sup> loading time constant (Fig. 3A, middle;  $2.4 \pm 0.5$  s in control and  $2.1 \pm 0.3$  s in the undercut group,  $P > 0.05$ ). There was a greater positive shift in  $E_{Cl}$  in the control group than in the undercut group in the first 3 s after the beginning of Cl<sup>-</sup> loading; however, the difference between the two groups did not reach a significant level ( $P = 0.055$ , Fig. 3C). These effects of furosemide suggest that the decreased chloride extrusion capability in undercut cells is likely due to reduced expression of KCC2. Furosemide also significantly reduced  $E_{Cl}$  recovery 10 s after the end of Cl<sup>-</sup> loading in both control and undercut groups (Fig. 3C, 10-s recovery and 10-s recovery in furo). The recovery time constant in 0.5 mM furosemide could not be accurately determined because the mean  $E_{Cl}$  recovery was only  $-2$  to  $-3$  mV.

#### $E_{Cl}$ in layer V pyramidal neurons of undercut and control cortex during whole cell recording

Another approach for testing the capacity of neurons to regulate  $[Cl^-]_i$  is to use a whole cell recording pipette to load the neurons with a known Cl<sup>-</sup> concentration and measure  $E_{Cl}$  under steady-state conditions. Because of the action of KCC2 to continuously pump out intracellular Cl<sup>-</sup>,  $E_{Cl}$  measured in whole cell recordings tends to be more negative than the predicted value, when the Cl<sup>-</sup> concentration in the pipette is high (20 and 40 mM) (DeFazio et al. 2000). We obtained whole cell recordings with patch pipettes containing 40 mM Cl<sup>-</sup> and used voltage ramps and muscimol application as above to measure  $E_{Cl}$  (e.g., Fig. 2B). Recording pipettes with resistance of 2.5–4 M $\Omega$  were used. There was no significant difference between the two groups in access resistance ( $9.5 \pm 0.5$  M $\Omega$  in control and  $10.8 \pm 0.5$  M $\Omega$  in undercut group,  $P > 0.05$ ). Acceptable whole cell recordings were obtained from 19 cells in 15 slices of control cortex from 9 rats and 18 neurons in 16 slices of undercut cortex from 8 rats.  $E_{Cl}$  was  $-53.4 \pm 1.2$  mV ( $n = 19$ ) and  $-49.8 \pm 0.6$  mV ( $n = 18$ ) after correction for liquid junction potential in control and undercut groups, respectively, values that were more negative than the predicted  $E_{Cl}$  of  $-29.8$  mV based on the Cl<sup>-</sup> concentrations in the pipette and ACSF, and the GHK equation. However, there was no significant difference in  $E_{Cl}$  between the control and undercut groups (Fig. 4;  $P > 0.05$ ; Mann-Whitney rank sum test was used because of unequal sample variance), a result similar to that obtained with perforated-patch recordings.

#### Blocking NKCC1 had no effect on $E_{Cl}$

One possible explanation for the lack of effect of injury on  $[Cl^-]_i$  and  $E_{Cl}$  in pyramidal neurons within the undercut cortex would be a concurrent decrease in both the outward Cl<sup>-</sup> cotransporter KCC2 and the inward Cl<sup>-</sup> cotransporter, NKCC1. Because the two cotransporters have opposite effects on  $[Cl^-]_i$ , downregulation of both might result in no change in  $[Cl^-]_i$  and  $E_{Cl}$ . To rule out this possibility, we examined the effect of bumetanide (10  $\mu$ M), which selectively inhibits NKCC1 at low concentrations (Beck et al. 2003; Russell 2000). Bumetanide application did not significantly affect  $E_{Cl}$  in neurons of either the control or undercut group under resting conditions (Fig. 5, left), 30 s after Cl<sup>-</sup> loading, or after 30 s recovery (Fig. 5, middle and right), suggesting that NKCC1 contributes little to the regulation of  $[Cl^-]_i$  in somata of adult layer V pyramidal cells. Bumetanide application did not affect the time constants of Cl<sup>-</sup> loading and recovery. Results are consistent with those of other studies showing that NKCC1 has a predominant dendritic localization and bumetanide does not affect  $E_{Cl}$  in somatically recorded mature pyramidal neurons (Martina et al. 2001; Marty et al. 2002).

#### $E_{Cl}$ in neonatal layer V pyramidal neurons

To confirm that our perforated-patch clamp recordings could correctly detect a change in  $E_{Cl}$ , if present, we used voltage ramps ranging from  $-90$  to  $-20$  mV to measure  $E_{Cl}$  of layer V pyramidal neurons in rat neocortical slices at P2–P6. At these times, the expression of KCC2 is markedly less than in mature cortex and  $E_{Cl}$  is known to be depolarized with respect to  $V_m$  (DeFazio et al. 2000; Owens et al. 1996; Yamada et al. 2004). The average  $V_m$  was  $-62.0 \pm 1.6$  mV and  $E_{Cl}$  was  $-56.3 \pm 1.3$  mV ( $n = 16$ ) or  $5.7 \pm 1.7$  mV more positive than  $V_m$  (Fig. 6). When the neurons were voltage-clamped at  $-30$  mV, Cl<sup>-</sup> loading caused a significant positive shift in  $E_{Cl}$  ( $E_{Cl} =$

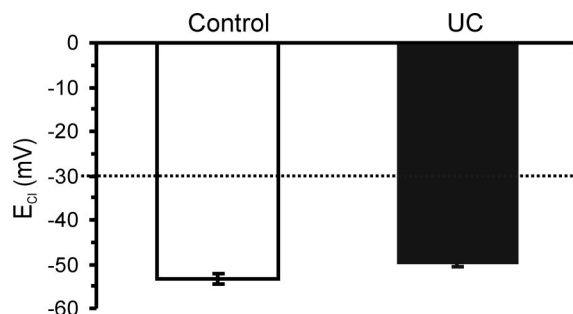


FIG. 4.  $E_{Cl}$  in whole cell recordings is similar in undercut vs. control animals. Reversal potentials for GABA<sub>A</sub> currents were recorded in layer V pyramidal cells with patch pipettes containing 40 mM Cl<sup>-</sup> during perfusion with ACSF containing 130 mM Cl<sup>-</sup>. Dashed line,  $E_{Cl}$  calculated from these values. More negative average values for  $E_{Cl}$  estimated from GABA reversal potentials were not significantly different between the control ( $n = 19$ ) and the undercut groups ( $n = 18$ ).

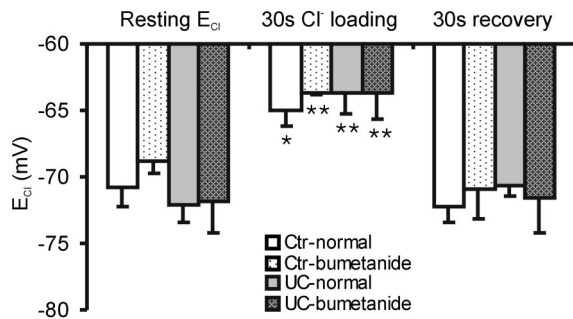


FIG. 5. Bumetanide has no effects on  $E_{\text{Cl}}$ .  $E_{\text{Cl}}$  was measured in layer V pyramidal neurons using perforated patch with or without the application of  $10 \mu\text{M}$  bumetanide in the control and undercut groups. There were no statistical differences between the 2 groups in resting  $E_{\text{Cl}}$  (left),  $E_{\text{Cl}}$  after 30-s  $\text{Cl}^-$  loading (middle), and during the recovery phase (right), in control ACSF or during application of  $10 \mu\text{M}$  bumetanide ( $n = 3-5$ ). However, there were significant (\*:  $P < 0.05$ ) or highly significant differences (\*\*:  $P < 0.01$ ) between resting  $E_{\text{Cl}}$  and  $E_{\text{Cl}}$  after 30-s  $\text{Cl}^-$  loading (middle), indicating the  $\text{Cl}^-$  loading protocol was effective.

$-40.9 \pm 1.8 \text{ mV}$ ,  $P < 0.0005$  when compared with resting  $E_{\text{Cl}}$ , indicating that the perforated recording method could reliably monitor changes in intracellular chloride. The positive shift in  $E_{\text{Cl}}$  did not recover in 30 s as in adult neurons. Rather a slow recovery of  $E_{\text{Cl}}$  to baseline values of  $-57.4 \pm 5.0 \text{ mV}$  occurred over 3–5 min, likely attributable to the effect of Donnan equilibrium.

## DISCUSSION

Our results indicate that neurons in epileptogenic partially isolated cortex maintain a normal resting  $E_{\text{Cl}}$ , even though the expression of KCC2 is reduced. This finding differs from several reports showing decreased KCC2 expression coupled with a depolarizing chloride reversal potential under various pathological conditions such as axotomy of facial and dorsal vagal motor neurons (Nabekura et al. 2002; Toyoda et al. 2003) or lamina I neurons of the spinal cord dorsal horn (Coull et al. 2003). Animals deficient in KCC2 exhibit an excitatory GABA and glycine action and frequent generalized seizures (Hubner et al. 2001; Woo et al. 2002), and seizure activity per se in the hippocampal kindling model causes downregulation of KCC2 and a depolarizing shift in  $E_{\text{Cl}}$  (Rivera et al. 2002). Reduction in KCC2 expression that leads to high  $[\text{Cl}^-]_i$  and depolarizing GABA<sub>A</sub> responses is thus a potential mechanism contributing to neuronal dysfunction in pathological conditions such as neuronal trauma and epilepsy.

There are several possible explanations for the lack of effects of this chronic injury on resting  $E_{\text{Cl}}$  in our experiments. First, as we did not measure KCC2 in the recorded neurons, it is possible that selection bias in some way resulted in sampling of cells in the partially isolated cortex that were less injured and had more normal KCC2 levels. For example, it might be more likely to obtain a satisfactory tight seal during patch-clamp recordings from such healthier neurons. This is a potential drawback generic to patch clamp studies of neurons in areas of CNS injury. The location of undercutting lesions just beneath layer VI suggests that most layer V pyramidal cells were axotomized, making it unlikely that our sample from partial isolations included a significant number of uninjured neurons. Another possible explanation for this discrepancy is a functional compensatory alteration of the KCC2 cotransporter

(see DISCUSSION below). One major difference between the undercut model employed here and previous studies of acute axotomy or other traumatic lesions is the chronic nature of the partial isolation. The delay of 2 wk between the injury and electrophysiological experiments would allow cortical neurons to recover from acute injury and compensatory mechanisms to potentially take place. Both the expression and level of activity of KCC2 are regulated by processes that may be altered by injury. NKCC and KCC2 activities in several nonneuronal cell types (Jennings 1999; Krarup et al. 1998; Lauf and Adragna 2000; Russell 2000) and in CNS neurons (Kelsch et al. 2001) can be modulated by phosphorylation–dephosphorylation mechanisms, by cAMP-dependent processes (Greger et al. 1999) and by myosin chain kinase (Kelley et al. 2000). Compensatory changes in one of these regulatory mechanisms might allow relatively normal KCC2 function at rest even though the expression of KCC2 is reduced.

## KCC2 and impaired $\text{Cl}^-$ extrusion

In the CNS, several anion transporters including  $\text{Na}^+ \text{--} \text{K}^+ \text{--} 2\text{Cl}^-$  (NKCC) cotransporter, the  $\text{K}^+ \text{--} \text{Cl}^-$  cotransporter (KCC),  $\text{Cl}^-/\text{HCO}_3^-$  exchanger and  $\text{Na}^+$ -coupled  $\text{Cl}^-/\text{HCO}_3^-$  exchanger act in concert to regulate intracellular pH and the concentration of anions (Chesler 2003; Payne et al. 2003). KCC2 is the major chloride cotransporter involved in maintaining low intracellular chloride concentration in adult neurons (Jarolimek et al. 1999; Kakazu et al. 1999; Rivera et al. 1999). When  $[\text{Cl}^-]_i$  is extremely low, or  $[\text{K}^+]_o$  is high, KCC2 can function in reverse and serves to move  $\text{Cl}^-$  into neurons (DeFazio et al. 2000; Payne 1997). NKCC1 expression is largely limited to dendritic regions where its activity results in accumulation of chloride ions, whereas in adult pyramidal neurons its expression is undetectable and contributes little to chloride homeostasis (Martina et al. 2001; Plotkin et al. 1997; Yamada et al. 2004). Other cotransporters such as  $\text{Cl}^-/\text{HCO}_3^-$  and  $\text{Na}^+$ -coupled  $\text{Cl}^-/\text{HCO}_3^-$  exchangers function in control of pH and are less involved in  $[\text{Cl}^-]_i$  regulation (Brett et al. 2002; Chesler 2003; Kaila 1994; Payne et al. 2003; Raley-Susman et al. 1993).

Reduced KCC2 expression often results in a positive shift in  $E_{\text{Cl}}$ , as has been shown in neuronal injuries and in other

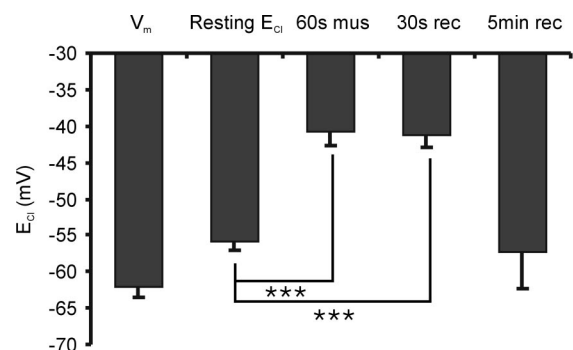


FIG. 6. Depolarized  $E_{\text{Cl}}$  in neonatal layer V pyramidal neurons.  $E_{\text{Cl}}$  was measured from P2 to P6 rats using perforated patch.  $E_{\text{Cl}}$  ( $-56.3 \pm 1.3 \text{ mV}$ ) was depolarized by  $5.7 \pm 1.7 \text{ mV}$  relative to  $V_m$  ( $-62.0 \pm 1.6 \text{ mV}$ ,  $n = 16$ ). When the neurons were held at  $-30 \text{ mV}$ ,  $\text{Cl}^-$  loading (60-s muscimol) caused a significant positive shift in  $E_{\text{Cl}}$  ( $E_{\text{Cl}} = -40.9 \pm 1.8 \text{ mV}$ , \*\*\*:  $P < 0.001$ , when compared with resting  $E_{\text{Cl}}$ ,  $n = 6$ ). This positive shift remained for  $>30 \text{ s}$  (30-s rec) but recovered to resting  $E_{\text{Cl}}$  level after 5 min (5 min rec).

epilepsy models (Coull et al. 2003; Malek et al. 2003; Nabekura et al. 2002; Toyoda et al. 2003). Our experiments were designed to determine whether similar reductions in KCC2 in layer V pyramidal neurons of partially isolated cortex (I. Parada, L. Kao, and D. A. Prince, unpublished observations) affected  $[Cl^-]_i$  regulation. We did not see a shift in baseline  $E_{Cl}$  in this model, perhaps because there is sufficient residual KCC2 in neurons to maintain  $Cl^-$  homeostasis under resting conditions when intense GABAergic activity is not present. However, the faster time constant and larger positive shift in  $E_{Cl}$  during the initial loading phase (Fig. 3) indicate that there is a more rapid rise in  $[Cl^-]_i$  during intense GABA<sub>A</sub> receptor activation in neurons of the partially isolated cortex. A decrease in somatic size, known to occur in corticospinal pyramidal neurons after axotomy (Tseng and Prince 1996) and pyramidal cells in partial isolations (Prince and Tseng 1993; and see above), cannot underlie this abnormality because both the calculated amount of  $Cl^-$  loading and the time constant of  $Cl^-$  loading in furosemide were not significantly different in control and undercut cells (Fig. 3A). From Fig. 3A, it is also evident that furosemide had little effect on the time constant of  $Cl^-$  loading in neurons of the undercut, while significantly speeding loading in control cells. Thus the loss of a furosemide-sensitive mechanism in the injured neurons underlies the decrease in time constant. Although low concentrations of furosemide inhibit  $\alpha 6$  subunit-containing GABA<sub>A</sub> receptors (Thompson et al. 1999), the expression of these receptors is highly limited to granule cells in the cerebellum (Pirker et al. 2000; Wisden et al. 1992), making it unlikely that the 0.5 mM furosemide used in our experiments would have significant direct effects on neocortical GABA<sub>A</sub> receptors. To the extent that furosemide, at the concentration employed, is selective for blockade of KCC2-mediated effects on  $Cl^-$  (DeFazio et al. 2000; Payne 1997), the findings indicate a functional reduction in the transporter. The observation that the amount of  $Cl^-$  loading was the same in control and undercut neurons also argues against a large difference in the density or function of GABA<sub>A</sub> receptors contributing to the more effective initial loading in the undercut cells, a conclusion further supported by the fact that the conductance induced by GABA puffs was similar in control and undercut cortical neurons (Table 1). The contrast between the normal  $E_{Cl}$  under resting conditions and the changes seen during intense activation of GABA<sub>A</sub> receptors in the chronically injured cells emphasizes the importance of assessing dynamic inhibitory function under physiological stress before concluding that inhibition is "normal." Changes in GABA transporter GAT-1 or -3 expression have been shown in several epilepsy models (Conti et al. 2004; During et al. 1995). Decrease in GAT-1 or -3 in undercut cortex could contribute to the faster  $Cl^-$  loading time constant by increasing GABA exposure and promoting GABA<sub>A</sub> channel activation. However, the calculated  $Cl^-$  load was not significantly different between the undercut and control groups, suggesting that changes in GABA transporters, even if present, did not contribute significantly to the difference in  $Cl^-$  loading time constant.

An increase in the time constant for recovery of  $E_{Cl}$  after  $Cl^-$  loading, which might have been expected in undercut cells with decreased KCC2 (e.g., Thompson et al. 1988), was not observed (Fig. 3). This result is consistent with the presence of sufficient residual KCC2 activity in undercut neurons to main-

tain a normal  $E_{Cl}$  under resting conditions or when the increase in  $[Cl^-]_i$  is small and protracted as during the recovery phase.  $Cl^-$  loading was most effective during the first few muscimol puffs; however, the effects of subsequent applications on membrane conductance decreased dramatically, likely due to desensitization of the GABA<sub>A</sub> receptor. This would tend to make  $Cl^-$  loading inefficient so that the residual capacity of the cell to extrude  $Cl^-$  would not be exceeded even though KCC2 was reduced. However, a rapid influx of large amounts of  $Cl^-$ , as occurred during the early phase of muscimol applications, uncovered a measurable reduction in  $Cl^-$  extrusion, presumably due to insufficiency of KCC2 activity in neurons of the undercut cortex. The lack of a significant difference in  $E_{Cl}$  between the undercut and control groups during whole cell recordings (Fig. 4) may likewise be due to a relatively slow diffusion of  $Cl^-$  from the pipette into the cell.

Because application of bumetanide did not affect resting  $E_{Cl}$ ,  $Cl^-$  loading, or recovery in either control or undercut cells (Fig. 5), a concurrent injury-induced alteration in the inward transporter, NKCC, is unlikely as a factor influencing our results. This conclusion is compatible with results of previous studies showing that changes in NKCC1 mRNA expression do not occur in acutely axotomized neurons (Nabekura et al. 2002; Toyoda et al. 2003). Thus we conclude that changes in the time constant of  $Cl^-$  loading and loss of furosemide efficacy in undercut neurons is attributable to a reduced  $Cl^-$  extrusion mechanism likely resulting from reduced KCC2 expression.

#### *Significance of impaired $Cl^-$ homeostasis*

A constant balance between excitation and inhibition is essential for the maintenance of normal cortical function. Repetitive activation of fast inhibitory events results in intracellular accumulation of chloride and depression of inhibition (Huguenard and Alger 1986; Ling and Benardo 1995; McCarren and Alger 1985; Thompson and Gahwiler 1989), and a reduction in inhibition is a major mechanism contributing to the generation of epileptiform discharge (Kobayashi and Buckmaster 2003; Mody et al. 1994; Rice et al. 1996). Our results indicate that layer V pyramidal neurons in the undercut cortex maintain a normal  $E_{Cl}$  under resting conditions. However, the faster, furosemide-sensitive time constant during early  $Cl^-$  loading (Fig. 3C) suggests that these neurons cannot clear chloride influx efficiently during intense inhibitory activity. GABAergic interneurons are relatively preserved in some chronic models of epileptogenesis (Babb et al. 1989; Magloczky et al. 2000; Prince et al. 1997) and can fire at high frequencies during epileptiform activity (Timofeev et al. 2002; Tuff et al. 1983; Velazquez and Carlen 1999; Wu and Leung 2001). Considering the much higher frequency of spontaneous synaptic activity in vivo (Pare et al. 1997), neurons in the epileptogenic cortex might encounter more intense GABAergic inhibition, resulting in larger  $Cl^-$  influxes and a more positive  $E_{Cl}$ . During epileptiform discharges, large increases in  $[K^+]_o$  occur (Moody et al. 1974); this would not only directly increase neuronal excitability but might also further increase  $[Cl^-]_i$  through reversed  $Cl^-$  transport by the partially impaired KCC2 (Payne 1997). Under these conditions, impaired  $Cl^-$  extrusion may result in large increases in  $[Cl^-]_i$ , convert hyperpolarizing GABAergic responses into depolarizing ones and enhance  $Ca^{2+}$  entry, thus contributing to the generation of

sustained depolarizations in networks of pyramidal neurons that contribute to epileptiform activities.

#### GRANTS

This work was supported by National Institute of Neurological Disorders and Stroke Grant NS-12151 and the Pimley research and training funds.

#### REFERENCES

- Andersen P, Dingledine R, Gjerstad L, Langmoen IA, and Laursen AM. Two different responses of hippocampal pyramidal cells to application of gamma-amino butyric acid. *J Physiol* 305: 279–296, 1980.
- Babb TL, Pretorius JK, Kupfer WR, and Crandall PH. Glutamate decarboxylase-immunoreactive neurons are preserved in human epileptic hippocampus. *J Neurosci* 9: 2562–2574, 1989.
- Beck J, Lenart B, Kintner DB, and Sun D. Na-K-Cl cotransporter contributes to glutamate-mediated excitotoxicity. *J Neurosci* 23: 5061–5068, 2003.
- Ben Ari Y, Tseeb V, Ragozzino D, Khazipov R, and Gaiarsa JL. gamma-Aminobutyric acid (GABA): a fast excitatory transmitter which may regulate the development of hippocampal neurones in early postnatal life. *Prog Brain Res* 102: 261–273, 1994.
- Benardo LS. Separate activation of fast and slow inhibitory postsynaptic potentials in rat neocortex in vitro. *J Physiol* 476: 203–215, 1994.
- Bernard C, Cossart R, Hirsch JC, Esclapez M, and Ben Ari Y. What is GABAergic inhibition? How is it modified in epilepsy? *Epilepsia* 41, Suppl 6: S90–S95, 2000.
- Bianchi MT, Song L, Zhang H, and Macdonald RL. Two different mechanisms of disinhibition produced by GABA<sub>A</sub> receptor mutations linked to epilepsy in humans. *J Neurosci* 22: 5321–5327, 2002.
- Bloom FE and Iversen LL. Localizing 3H-GABA in nerve terminals of rat cerebral cortex by electron microscopic autoradiography. *Nature* 229: 628–630, 1971.
- Bormann J, Hamill OP, and Sakmann B. Mechanism of anion permeation through channels gated by glycine and gamma-aminobutyric acid in mouse cultured spinal neurones. *J Physiol* 385: 243–286, 1987.
- Brett CL, Kelly T, Sheldon C, and Church J. Regulation of  $\text{Cl}^-/\text{HCO}_3^-$  exchangers by cAMP-dependent protein kinase in adult rat hippocampal CA1 neurons. *J Physiol* 545: 837–853, 2002.
- Buckmaster PS and Jongen-Relo AL. Highly specific neuron loss preserves lateral inhibitory circuits in the dentate gyrus of kainate-induced epileptic rats. *J Neurosci* 19: 9519–9529, 1999.
- Chagnac-Amitai Y and Connors BW. Horizontal spread of synchronized activity in neocortex and its control by GABA-mediated inhibition. *J Neurophysiol* 61: 747–758, 1989.
- Cherubini E, Rovira C, Gaiarsa JL, Corradetti R, and Ben Ari Y. GABA mediated excitation in immature rat CA3 hippocampal neurons. *Int J Dev Neurosci* 8: 481–490, 1990.
- Chesler M. Regulation and modulation of pH in the brain. *Physiol Rev* 83: 1183–1221, 2003.
- Clayton GH, Owens GC, Wolff JS, and Smith RL. Ontogeny of cation- $\text{Cl}^-$  cotransporter expression in rat neocortex. *Brain Res Dev Brain Res* 109: 281–292, 1998.
- Connors BW, Gutnick MJ, and Prince DA. Electrophysiological properties of neocortical neurons in vitro. *J Neurophysiol* 48: 1302–1320, 1982.
- Connors BW, Malenka RC, and Silva LR. Two inhibitory postsynaptic potentials, and GABA<sub>A</sub> and GABA<sub>B</sub> receptor-mediated responses in neocortex of rat and cat. *J Physiol* 406: 443–468, 1988.
- Conti F, Minelli A, and Melone M. GABA transporters in the mammalian cerebral cortex: localization, development and pathological implications. *Brain Res Brain Res Rev* 45: 196–212, 2004.
- Coull JA, Boudreau D, Bachand K, Prescott SA, Nault F, Sik A, De Koninck P, and De Koninck Y. Trans-synaptic shift in anion gradient in spinal lamina I neurons as a mechanism of neuropathic pain. *Nature* 424: 938–942, 2003.
- Dallwig R, Deitmer JW, and Backus KH. On the mechanism of GABA-induced currents in cultured rat cortical neurons. *Pfluegers* 437: 289–297, 1999.
- DeFazio RA, Keros S, Quick MW, and Hablitz JJ. Potassium-coupled chloride cotransport controls intracellular chloride in rat neocortical pyramidal neurons. *J Neurosci* 20: 8069–8076, 2000.
- Dinocourt C, Petanjek Z, Freund TF, Ben Ari Y, and Esclapez M. Loss of interneurons innervating pyramidal cell dendrites and axon initial segments in the CA1 region of the hippocampus following pilocarpine-induced seizures. *J Comp Neurol* 459: 407–425, 2003.
- During MJ, Ryder KM, and Spencer DD. Hippocampal GABA transporter function in temporal-lobe epilepsy. *Nature* 376: 174–177, 1995.
- Echlin FA and Battista A. Epileptiform seizures from chronic isolated cortex. *Arch Neurol* 168: 154–170, 1963.
- Graber KD and Prince DA. Tetrodotoxin prevents posttraumatic epileptogenesis in rats. *Ann Neurol* 46: 234–242, 1999.
- Greger R, Heitzmann D, Hug MJ, Hoffmann EK, and Bleich M. The  $\text{Na}^+2\text{Cl}^-K^+$  cotransporter in the rectal gland of *Squalus acanthias* is activated by cell shrinkage. *Pfluegers* 438: 165–176, 1999.
- Hoffman SN, Salin PA, and Prince DA. Chronic neocortical epileptogenesis in vitro. *J Neurophysiol* 71: 1762–1773, 1994.
- Hubner CA, Stein V, Hermans-Borgmeyer I, Meyer T, Ballanyi K, and Jentsch TJ. Disruption of KCC2 reveals an essential role of K-Cl cotransport already in early synaptic inhibition. *Neuron* 30: 515–524, 2001.
- Huguenard JR and Alger BE. Whole-cell voltage-clamp study of the fading of GABA-activated currents in acutely dissociated hippocampal neurons. *J Neurophysiol* 56: 1–18, 1986.
- Jerolimik W, Lewen A, and Misgeld U. A furosemide-sensitive  $\text{K}^+$ - $\text{Cl}^-$  cotransporter counteracts intracellular  $\text{Cl}^-$  accumulation and depletion in cultured rat midbrain neurons. *J Neurosci* 19: 4695–4704, 1999.
- Jennings ML. Volume-sensitive  $\text{K}^+/\text{Cl}^-$  cotransport in rabbit erythrocytes. Analysis of the rate-limiting activation and inactivation events. *J Gen Physiol* 114: 743–758, 1999.
- Kaila K. Ionic basis of GABA<sub>A</sub> receptor channel function in the nervous system. *Prog Neurobiol* 42: 489–537, 1994.
- Kaila K, Voipio J, Paalasmaa P, Pasternack M, and Deisz RA. The role of bicarbonate in GABA<sub>A</sub> receptor-mediated IPSPs of rat neocortical neurones. *J Physiol* 464: 273–289, 1993.
- Kakazu Y, Akaike N, Komiyama S, and Nabekura J. Regulation of intracellular chloride by cotransporters in developing lateral superior olive neurons. *J Neurosci* 19: 2843–2851, 1999.
- Kelley SJ, Thomas R, and Dunham PB. Candidate inhibitor of the volume-sensitive kinase regulating K-Cl cotransport: the myosin light chain kinase inhibitor ML-7. *J Membr Biol* 178: 31–41, 2000.
- Kelsch W, Hormuzdi S, Straube E, Lewen A, Monyer H, and Misgeld U. Insulin-like growth factor 1 and a cytosolic tyrosine kinase activate chloride outward transport during maturation of hippocampal neurons. *J Neurosci* 21: 8339–8347, 2001.
- Kobayashi M and Buckmaster PS. Reduced inhibition of dentate granule cells in a model of temporal lobe epilepsy. *J Neurosci* 23: 2440–2452, 2003.
- Krupp T, Jakobsen LD, Jensen BS, and Hoffmann EK.  $\text{Na}^+K^+2\text{Cl}^-$  cotransport in Ehrlich cells: regulation by protein phosphatases and kinases. *Am J Physiol Cell Physiol* 275: C239–C250, 1998.
- Kumar SS, Bacci A, Kharazia V, and Huguenard JR. A developmental switch of AMPA receptor subunits in neocortical pyramidal neurons. *J Neurosci* 22: 3005–3015, 2002.
- Lauf PK and Adragna NC. K-Cl cotransport: properties and molecular mechanism. *Cell Physiol Biochem* 10: 341–354, 2000.
- Li H and Prince DA. Synaptic activity in chronically injured, epileptogenic sensory-motor neocortex. *J Neurophysiol* 88: 2–12, 2002.
- Ling DS and Benardo LS. Recruitment of GABA<sub>A</sub> inhibition in rat neocortex is limited and not NMDA dependent. *J Neurophysiol* 74: 2329–2335, 1995.
- Luhmann HJ and Prince DA. Postnatal maturation of the GABAergic system in rat neocortex. *J Neurophysiol* 65: 247–263, 1991.
- Magloczky Z, Wittner L, Borhegyi Z, Halasz P, Vajda J, Czirjak S, and Freund TF. Changes in the distribution and connectivity of interneurons in the epileptic human dentate gyrus. *Neuroscience* 96: 7–25, 2000.
- Malek SA, Coderre E, and Stys PK. Aberrant chloride transport contributes to anoxic/ischemic white matter injury. *J Neurosci* 23: 3826–3836, 2003.
- Martina M, Royer S, and Pare D. Cell-type-specific GABA responses and chloride homeostasis in the cortex and amygdala. *J Neurophysiol* 86: 2887–2895, 2001.
- Marty A and Neher E. Potassium channels in cultured bovine adrenal chromaffin cells. *J Physiol* 367: 117–141, 1985.
- Marty S, Wehrle R, Alvarez-Leefmans FJ, Gasnier B, and Sotelo C. Postnatal maturation of  $\text{Na}^+$ ,  $\text{K}^+$ ,  $2\text{Cl}^-$  cotransporter expression and inhibitory synaptogenesis in the rat hippocampus: an immunocytochemical analysis. *Eur J Neurosci* 15: 233–245, 2002.
- McCarren M, and Alger BE. Use-dependent depression of IPSPs in rat hippocampal pyramidal cells in vitro. *J Neurophysiol* 53: 557–571, 1985.
- McCormick DA, Connors BW, Lighthall JW, and Prince DA. Comparative electrophysiology of pyramidal and sparsely spiny stellate neurons of the neocortex. *J Neurophysiol* 54: 782–806, 1985.

- Mikawa S, Wang C, Shu F, Wang T, Fukuda A, and Sato K.** Developmental changes in KCC1, KCC2 and NKCC1 mRNAs in the rat cerebellum. *Brain Res Dev Brain Res* 136: 93–100, 2002.
- Mody I, De Koninck Y, Otis TS, and Soltesz I.** Bridging the cleft at GABA synapses in the brain. *Trends Neurosci* 17: 517–525, 1994.
- Moody WJ, Futamachi KJ, and Prince DA.** Extracellular potassium activity during epileptogenesis. *Exp Neurol* 42: 248–263, 1974.
- Nabekura J, Ueno T, Okabe A, Furuta A, Iwaki T, Shimizu-Okabe C, Fukuda A, and Akaike N.** Reduction of KCC2 expression and GABA<sub>A</sub> receptor-mediated excitation after in vivo axonal injury. *J Neurosci* 22: 4412–4417, 2002.
- Okabe A, Ohno K, Toyoda H, Yokokura M, Sato K, and Fukuda A.** Amygdala kindling induces upregulation of mRNA for NKCC1, a Na(+), K(+)-2Cl(-) cotransporter, in the rat piriform cortex. *Neurosci Res* 44: 225–229, 2002.
- Owens DF, Boyce LH, Davis MB, and Kriegstein AR.** Excitatory GABA responses in embryonic and neonatal cortical slices demonstrated by gramicidin perforated-patch recordings and calcium imaging. *J Neurosci* 16: 6414–6423, 1996.
- Pare D, Lebel E, and Lang EJ.** Differential impact of miniature synaptic potentials on the soma and dendrites of pyramidal neurons in vivo. *J Neurophysiol* 78: 1735–1739, 1997.
- Payne JA.** Functional characterization of the neuronal-specific K-Cl cotransporter: implications for [K<sup>+</sup>]<sub>o</sub> regulation. *Am J Physiol Cell Physiol* 273: C1516–C1525, 1997.
- Payne JA, Rivera C, Voipio J, and Kaila K.** Cation-chloride co-transporters in neuronal communication, development and trauma. *Trends Neurosci* 26: 199–206, 2003.
- Pirker S, Schwarzer C, Wieselthaler A, Sieghart W, and Sperk G.** GABA(A) receptors: immunocytochemical distribution of 13 subunits in the adult rat brain. *Neuroscience* 101: 815–850, 2000.
- Plotkin MD, Snyder EY, Hebert SC, and Delpire E.** Expression of the Na-K-2Cl cotransporter is developmentally regulated in postnatal rat brains: a possible mechanism underlying GABA's excitatory role in immature brain. *J Neurobiol* 33: 781–795, 1997.
- Prince DA.** Epileptogenic neurons and circuits. *Adv Neurol* 79: 665–684, 1999.
- Prince DA, Jacobs KM, Salin P, Hoffman S, and Parada I.** Chronic focal neocortical epileptogenesis: does disinhibition play a role? *Can J Physiol Pharmacol* 75: 500–507, 1997.
- Prince DA, Kao L, and Parada I.** Decrease in the potassium/chloride cotransporter KCC2 in chronically injured epileptogenic neocortex. *Society for Neuroscience Annual Meeting* 2000.
- Prince DA and Tseng GF.** Epileptogenesis in chronically injured cortex: in vitro studies. *J Neurophysiol* 69: 1276–1291, 1993.
- Raley-Susman KM, Sapolsky RM, and Kopito RR.** Cl<sup>-</sup>/HCO<sub>3</sub><sup>-</sup> exchange function differs in adult and fetal rat hippocampal neurons. *Brain Res* 614: 308–314, 1993.
- Rall W.** Core conductor theory and cable properties of neurons. In: *Handbook of Physiology. The Nervous System. Cellular Biology of Neurons*. Bethesda, MD: Am Physiol Soc 1977, sect. 1, vol. I, p. 39–97.
- Ribak CE, Bradburne RM, and Harris AB.** A preferential loss of GABAergic, symmetric synapses in epileptic foci: a quantitative ultrastructural analysis of monkey neocortex. *J Neurosci* 2: 1725–1735, 1982.
- Rice A, Rafiq A, Shapiro SM, Jakoi ER, Coulter DA, and DeLorenzo RJ.** Long-lasting reduction of inhibitory function and gamma-aminobutyric acid type A receptor subunit mRNA expression in a model of temporal lobe epilepsy. *Proc Natl Acad Sci USA* 93: 9665–9669, 1996.
- Rivera C, Li H, Thomas-Crusells J, Lahtinen H, Viitanen T, Nanobashvili A, Kokaia Z, Airaksinen MS, Voipio J, Kaila K, and Saarma M.** BDNF-induced TrkB activation down-regulates the K<sup>+</sup>-Cl<sup>-</sup> cotransporter KCC2 and impairs neuronal Cl<sup>-</sup> extrusion. *J Cell Biol* 159: 747–752, 2002.
- Rivera C, Voipio J, Payne JA, Ruusuvoori E, Lahtinen H, Lamsa K, Pirvola U, Saarma M, and Kaila K.** The K<sup>+</sup>/Cl<sup>-</sup> co-transporter KCC2 renders GABA hyperpolarizing during neuronal maturation. *Nature* 397: 251–255, 1999.
- Roper SN, King MA, Abraham LA, and Boillot MA.** Disinhibited in vitro neocortical slices containing experimentally induced cortical dysplasia demonstrate hyperexcitability. *Epilepsy Res* 26: 443–449, 1997.
- Russell JM.** Sodium-potassium-chloride cotransport. *Physiol Rev* 80: 211–276, 2000.
- Salin P, Tseng GF, Hoffman S, Parada I, and Prince DA.** Axonal sprouting in layer V pyramidal neurons of chronically injured cerebral cortex. *J Neurosci* 15: 8234–8245, 1995.
- Schwartzkroin PA and Prince DA.** Cellular and field potential properties of epileptogenic hippocampal slices. *Brain Res* 147: 117–130, 1978.
- Scoville WB.** Late results of orbital undercutting. Report of 76 patients undergoing quantitative selective lobotomies. *Am J Psychiatry* 117: 525–532, 1960.
- Sharpless SK and Halpern LM.** The electrical excitability of chronically isolated cortex studied by means of permanently implanted electrodes. *Electroencephalogr Clin Neurophysiol* 14: 244–255, 1962.
- Sloviter RS.** Decreased hippocampal inhibition and a selective loss of interneurons in experimental epilepsy. *Science* 235: 73–76, 1987.
- Staley KJ and Proctor WR.** Modulation of mammalian dendritic GABA(A) receptor function by the kinetics of Cl<sup>-</sup> and HCO<sub>3</sub><sup>-</sup> transporter. *J Physiol* 519: 693–712, 1999.
- Staley KJ, Soldo BL, and Proctor WR.** Ionic mechanisms of neuronal excitation by inhibitory GABA<sub>A</sub> receptors. *Science* 269: 977–981, 1995.
- Sun QQ, Akk G, Huguenard JR, and Prince DA.** Differential regulation of GABA release and neuronal excitability mediated by neuropeptide Y1 and Y2 receptors in rat thalamic neurons. *J Physiol* 531: 81–94, 2001.
- Taira T, Lamsa K, and Kaila K.** Posttetanic excitation mediated by GABA<sub>A</sub> receptors in rat CA1 pyramidal neurons. *J Neurophysiol* 77: 2213–2218, 1997.
- Thompson SA, Arden SA, Marshall G, Wingrove PB, Whiting PJ, and Wafford KA.** Residues in transmembrane domains I and II determine gamma-aminobutyric acid type AA receptor subtype-selective antagonism by furosemide. *Mol Pharmacol* 55: 993–999, 1999.
- Thompson SM, Deisz RA, and Prince DA.** Relative contributions of passive equilibrium and active transport to the distribution of chloride in mammalian cortical neurons. *J Neurophysiol* 60: 105–124, 1988.
- Thompson SM and Gahwiler BH.** Activity-dependent disinhibition. I. Repetitive stimulation reduces IPSP driving force and conductance in the hippocampus in vitro. *J Neurophysiol* 61: 501–511, 1989.
- Timofeev I, Grenier F, and Steriade M.** The role of chloride-dependent inhibition and the activity of fast-spiking neurons during cortical spike-wave electrographic seizures. *Neuroscience* 114: 1115–1132, 2002.
- Toyoda H, Ohno K, Yamada J, Ikeda M, Okabe A, Sato K, Hashimoto K, and Fukuda A.** Induction of NMDA and GABA<sub>A</sub> receptor-mediated Ca<sup>2+</sup> oscillations with KCC2 mRNA downregulation in injured facial motoneurons. *J Neurophysiol* 89: 1353–1362, 2003.
- Tseng GF and Prince DA.** Structural and functional alterations in rat corticospinal neurons after axotomy. *J Neurophysiol* 75: 248–267, 1996.
- Tuff LP, Racine RJ, and Adamec R.** The effects of kindling on GABA-mediated inhibition in the dentate gyrus of the rat. I. Paired-pulse depression. *Brain Res* 277: 79–90, 1983.
- van den Pol AN, Obrietan K, and Chen G.** Excitatory actions of GABA after neuronal trauma. *J Neurosci* 16: 4283–4292, 1996.
- Velazquez JL and Carlen PL.** Synchronization of GABAergic interneuronal networks during seizure-like activity in the rat horizontal hippocampal slice. *Eur J Neurosci* 11: 4110–4118, 1999.
- Wallace RH, Marini C, Petrou S, Harkin LA, Bowser DN, Panchal RG, Williams DA, Sutherland GR, Mulley JC, Scheffer IE, and Berkovic SF.** Mutant GABA(A) receptor gamma2-subunit in childhood absence epilepsy and febrile seizures. *Nat Genet* 28: 49–52, 2001.
- Wisden W, Laurie DJ, Monyer H, and Seeburg PH.** The distribution of 13 GABA<sub>A</sub> receptor subunit mRNAs in the rat brain. I. Telencephalon, diencephalon, mesencephalon. *J Neurosci* 12: 1040–1062, 1992.
- Woo NS, Lu J, England R, McClellan R, Dufour S, Mount DB, Deutch AY, Lovinger DM, and Delpire E.** Hyperexcitability and epilepsy associated with disruption of the mouse neuronal-specific K-Cl cotransporter gene. *Hippocampus* 12: 258–268, 2002.
- Wu K and Leung LS.** Enhanced but fragile inhibition in the dentate gyrus in vivo in the kainic acid model of temporal lobe epilepsy: a study using current source density analysis. *Neuroscience* 104: 379–396, 2001.
- Yamada J, Okabe A, Toyoda H, Kilb W, Luhmann HJ, and Fukuda A.** Cl<sup>-</sup> uptake promoting depolarizing GABA actions in immature rat neocortical neurons is mediated by NKCC1. *J Physiol* 557: 829–841, 2004.
- Zilles KaWA.** Cortex: area and laminar structure. In: *The Rat Nervous System*, edited by G. Paxinos. Kensington, Australia: Academic, 1985, vol. I, p. 375–415.